

Naval Research Laboratory

Washington, DC 20375-5320



NRL/MR/6170--97-8103

Vanadate-sulfate Melt Thermochemistry Relating to Hot Corrosion of Thermal Barrier Coatings

ROBERT L. JONES

*Surface Chemistry Branch
Chemistry Division*

October 30, 1997

4100 QUALITY INSPECTED 4

Approved for public release; distribution is unlimited.

19980105 061

REPORT DOCUMENTATION PAGE

*Form Approved
OMB No. 0704-0188*

Public reporting burden for this collection of information is estimated to average 1 hour per response, including the time for reviewing instructions, searching existing data sources, gathering and maintaining the data needed, and completing and reviewing the collection of information. Send comments regarding this burden estimate or any other aspect of this collection of information, including suggestions for reducing this burden, to Washington Headquarters Services, Directorate for Information Operations and Reports, 1215 Jefferson Davis Highway, Suite 1204, Arlington, VA 22202-4302, and to the Office of Management and Budget, Paperwork Reduction Project (0704-0188), Washington, DC 20503.

1. AGENCY USE ONLY (Leave Blank)	2. REPORT DATE	3. REPORT TYPE AND DATES COVERED	
	October 30, 1997	Final Report	
4. TITLE AND SUBTITLE Vandate-sulfate Melt Thermochemistry Relating to Hot Corrosion of Thermal Barrier Coatings			5. FUNDING NUMBERS PE - 61153N PE - 62234N
6. AUTHOR(S) Robert L. Jones			
7. PERFORMING ORGANIZATION NAME(S) AND ADDRESS(ES) Naval Research Laboratory Washington, DC 20375-5320			8. PERFORMING ORGANIZATION REPORT NUMBER NRL/MR/6170-97-8103
9. SPONSORING/MONITORING AGENCY NAME(S) AND ADDRESS(ES) Office of Naval Research 800 North Quincy Street Arlington, VA 22217-5660			10. SPONSORING/MONITORING AGENCY REPORT NUMBER
11. SUPPLEMENTARY NOTES			
12a. DISTRIBUTION/AVAILABILITY STATEMENT Approved for public release; distribution unlimited.			12b. DISTRIBUTION CODE
13. ABSTRACT (Maximum 200 words) The gas turbine industry is moving strongly toward the use of ZrO ₂ -based thermal barrier coatings (TBCs) on hot section vanes/blades to increase engine efficiency and durability. In some applications (e.g., ship propulsion or electricity generation), such TBCs may be corroded by molten vanadate-sulfate deposits from fuel impurities. This Report provides a synopsis of vanadate-sulfate thermochemistry relating to TBC hot corrosion, and summarizes research conducted on this topic at the Naval Research Laboratory. The interactions of Na ₂ O, V ₂ O ₅ and SO ₃ , the melt components which determine the composition of the vanadate-sulfate deposits, were examined and clarified. Vanadate-sulfate melts were shown to be nonideal rather than ideal—a point of some contention in the past literature—and, for melts of Na/V = 1, to have a V ₂ O ₅ activity coefficient (γ) that ranges from 5×10^{-4} up to essentially 1, depending on the SO ₃ overpressure. Different NaVO ₃ /Na ₂ SO ₄ mixtures gave a detectable but small change in $\gamma(V_2O_5)$, suggesting that the Na/V ratio is relatively unimportant, for melts equilibrated with SO ₃ , in determining $\gamma(V_2O_5)$. The reactions of several candidate ZrO ₂ stabilizers (MgO, CeO ₂ , Sc ₂ O ₃ , In ₂ O ₃ , SnO ₂) with vanadate-sulfate melts are categorized and discussed.			
14. SUBJECT TERMS Hot corrosion Vanadate sulfate melts			15. NUMBER OF PAGES 23
			16. PRICE CODE
17. SECURITY CLASSIFICATION OF REPORT UNCLASSIFIED	18. SECURITY CLASSIFICATION OF THIS PAGE UNCLASSIFIED	19. SECURITY CLASSIFICATION OF ABSTRACT UNCLASSIFIED	20. LIMITATION OF ABSTRACT UL

CONTENTS

INTRODUCTION.....	1
GAS TURBINE VANE/BLADE TBCs.....	1
COMBINED CYCLE GAS TURBINES FOR ELECTRICITY GENERATION..	1
VANADIUM IN PETROLEUM.....	2
PREVIOUS STUDIES OF VANADATE HOT CORROSION OF TBCs.....	2
THERMOCHEMISTRY OF VANADATE-SULFATE MELTS: REVIEW AND DISCUSSION.....	3
MECHANISM OF VANADATE HOT CORROSION OF $\text{Y}_2\text{O}_3\text{-ZrO}_2$ TBCs...	3
LEWIS ACID/BASE REACTION OF CERAMIC OXIDES WITH SODIUM VANADATES.....	4
PREVIOUS STUDIES OF VANADATE-SULFATE THERMOCHEMISTRY..	5
QUESTION OF $\text{V}^{4+}/\text{V}^{5+}$ IN VANADATE-SULFATE MELTS.....	5
THERMODYNAMIC MODELING OF ACID-BASE MELTS.....	6
STUDY OF $\text{Na}_2\text{O-V}_2\text{O}_5$ MELTS BY MITTAL AND ELLIOTT.....	7
THERMOGRAVIMETRIC EQUILIBRIUM OF SO_3 WITH NaVO_3 MELTS....	9
THERMODYNAMIC ANALYSIS OF $\text{SO}_3\text{-NaVO}_3$ EQUILIBRIUM DATA....	10
REACTION OF CANDIDATE STABILIZING OXIDES WITH $\text{SO}_3\text{-NaVO}_3$...	12
DETERMINING ACT.(V_2O_5) WITHOUT ASSUMPTION AS TO ACT.(Na_2SO_4).....	14
V_2O_5 TITRATION USING CeVO_4 FORMATION AS "INDICATOR" TO DETERMINE $\gamma(\text{V}_2\text{O}_5)$	15
SUMMARY AND CONCLUSIONS.....	17
COMPARISON WITH V_2O_5 ACTIVITY COEFFICIENTS FROM THE LITERATURE.....	17
OTHER CONSIDERATIONS.....	18
ACKNOWLEDGEMENTS.....	18
REFERENCES.....	18

VANADATE-SULFATE MELT THERMOCHEMISTRY RELATING TO HOT CORROSION OF THERMAL BARRIER COATINGS

INTRODUCTION

The purpose of this Report is to draw together the knowledge of vanadate-sulfate thermochemistry relating to TBC hot corrosion, including that obtained in work done over several years in Code 6170 of the U.S. Naval Research Laboratory, and to present the total in reviewed form. This is important for several reasons. First, gas turbine technology is now moving toward the wide-spread use of TBCs on the 1st stage turbine vanes/blades (i.e., highly critical components), with many such TBC-fitted engines likely to be used for electricity-generation or other industrial/marine applications where V,S-containing fuels are possible. The hot corrosion of TBCs, and therefore the thermochemistry of vanadate-sulfate melts, may become of concern in these cases. Second, although there have been many thermodynamic studies of metallurgical slags, fused salts, silicate glasses, etc., surprisingly few investigations of vanadate-sulfate melts have been made, despite the long history of vanadate-sulfate hot corrosion (1). And third, among even these few studies, significant differences in findings have been reported. By defining these differences, it may be possible to identify areas in vanadate-sulfate thermochemistry where new research is needed.

Gas Turbine Vane/Blade TBCs

Zirconia is a high temperature thermal insulator, and a ZrO_2 "thermal barrier coating" as thin as 0.010" (0.25 mm) can reduce the temperature between the engine gas and component metal by 100-200°C. Many problems have had to be solved to make TBCs viable (2,3), especially for 1st stage turbine vanes (stationary) and blades (rotating) where large-scale TBC failure could jeopardize engine life. The TBC structure now commonly used for vane/blade applications (Fig. 1) consists of an 0.003-0.005" oxidation-resistant metallic "bond coat" of MCrAlY (where $M = \text{Co, Ni, or NiCo}$) or Pt-aluminide under a ~0.010" layer of Y_2O_3 (8-wt%)- ZrO_2 having a columnar, carpet pile-like physical structure. This columnar structure is produced by electron beam-physical vapor deposition (EB-PVD), and is thought to be essential for relieving thermal stress within the TBC, and so yielding long service life.

Significant advantages are claimed for TBCs on vanes/blades, including improved power (up to 20%), fuel economy (several percent), and/or component life (up to 3X improvement). For example, in land-based gas turbines, an increase of 55°C in turbine gas temperature is expected to provide an 8 to 13 percent gain in power, and a 1 to 4 percent increase in simple cycle efficiency (4). The faith of the gas turbine industry in TBC technology is shown by the fact that many \$10s of millions of dollars have been spent by such companies as United Technologies (Pratt & Whitney Aircraft Engines), General Electric Aircraft Engine Company, Chromalloy Corp., and Praxair Surface Technologies to purchase production-scale, EB-PVD coaters for application of TBCs to aviation and industrial gas turbine vanes/blades.

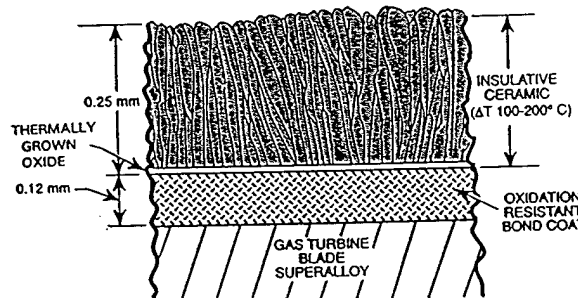


Fig. 1 Schematic drawing of EB-PVD thermal barrier coating.

Combined Cycle Gas Turbines for Electricity Generation

A world-wide movement is underway, as exemplified in the U.S. Dept. of Energy 8-year, \$700M Advanced Turbine Systems (ATS) Program (5), to use high efficiency gas turbines in combined cycle with bottoming steam turbines to produce electricity with up to 60% thermal efficiency. Such plants would require approximately 50% less fuel than present-day fired boiler plants which have 35-42% thermal efficiency. Moreover, since these plants are intended mostly to burn natural gas, which normally consists of 90% or more of methane (CH_4), there would be proportionately less CO_2 released to the environment than with fuels of higher C/H ratio.

To achieve high fuel efficiency, the massive electricity-generating gas turbines (with power in ranges of up to 250-300 MW) will employ the latest gas turbine technology, with many using single crystal blades (despite their large size) and TBC coated vanes/blades. Because of the possibility of future high prices, or shortages, in natural gas, these engines must have the back-up capability for firing with industrial-grade petroleum fuel. The vane/blade TBCs must therefore have the ability to withstand at least certain levels of vanadium and sulfur fuel impurities, even though the high surface temperatures for TBCs may tend to reduce deposit accumulation. Also, it is common in less developed countries to burn locally-produced industrial or crude oils that may contain significant vanadium or sulfur, and engine manufacturers are seeking vane/blade TBCs that can be used, with economic advantage, even in these circumstances.

Vanadium in Petroleum

Vanadium occurs in most crude oils, and in some cases, at levels up to 500 ppm (6). The vanadium is mostly complexed as heavy metalloporphyrin molecules, and tends to remain in the residual during refining; however, since metalloporphyrins are slightly volatile at higher temperatures, some vanadium may also be found in the higher-boiling distillate fuels.

Vanadium (as V_2O_6) accumulates on, and deactivates, the catalysts used in the fluid catalyst cracking of petroleum. Much effort has been spent to alleviate this problem, which is now mostly approached by catalyst modification, or metals passivation where certain metals such as Sb or Sn are added to the feedstock to "passivate" the catalyst against V_2O_6 attack (6,7). Vanadium also interferes with the hydrogen-desulfurization (HDS) of high-sulfur crudes by depositing on the catalyst. To remove vanadium itself, refiners can use an aggressive hydrogen treatment over catalysts (hydrodemetallization or HDM), as well as coking or other means (6). Approximately 2,650 metric tons of vanadium were recovered and marketed in the US from petroleum residues in 1996 (8). The treatments for removing vanadium are sophisticated and expensive, however, and may not be routinely performed in refining, especially in less developed countries.

Previous Studies of Vanadate Hot Corrosion of TBCs

During the fuel crises of the 1970s, the U.S. Dept. of Energy investigated alternative sources of liquid fossil fuel (coal liquefaction, etc.), as well as means for improving engine fuel economy (e.g., thermal barrier coatings). The possible corrosive attack of TBCs by low-quality alternate fuel containing vanadium, phosphorus, sulfur, etc. was investigated under DOE contract by several engine companies including Westinghouse, General Electric, Solar Turbines and others. The results from these studies were primarily published in two Conference Proceedings (9,10) jointly sponsored by DOE and EPRI (Electric Power Research Institute).

The DOE-sponsored studies focused essentially on MgO (20-25wt%)- ZrO_2 (MSZ) and Y_2O_3 (8-20wt%)- ZrO_2 (YSZ) thermal barrier coatings. MSZ was found to lack high temperature phase stability, and to be destabilized simply by thermal cycling to 1000°C. The MgO stabilizer, although somewhat

more resistant to reaction with V_2O_6 than Y_2O_3 , reacted readily with SO_3 to form $MgSO_4$, and was strongly leached from MSZ by the SO_3 in burner rigs burning 1wt%-S fuel. YSZ was clearly superior, and exhibited good 1000°C phase stability, as well as resistance to reaction with Na_2SO_4 - SO_3 at the SO_3 partial pressures found in engines burning fuel of 1-2% S levels. However, Y_2O_3 was confirmed by many as being highly reactive with V_2O_6 , even when the Y_2O_3 was at reduced activity as 8-wt% (4.5 mol%) Y_2O_3 in solid solution in ZrO_2 .

Building upon the original DOE-funded work, the U.S. Naval Sea Systems Command sponsored research to explore the potential of TBCs for vane/blade use in the General Electric LM2500 gas turbine which powers several important classes of Navy ships. Burner rig tests, along with one limited engine test, indicated that coatings of Y_2O_3 (8-wt%)- ZrO_2 in fact resisted $NaSO_4$ - SO_3 hot corrosion better than the metallic MCrAlY or Pt-aluminide coatings normally used for corrosion protection (11). There was also no evidence of molten salt penetration into the intergranular spacings of the EB-PVD prepared thermal barrier coatings. The relative performance of MgO -, CeO_2 -, and Y_2O_3 -stabilized ZrO_2 TBCs was evaluated in another burner rig test series, which used fuel contaminated with vanadium (up to ~90 ppm), sea salt, and sulfur (12). MgO - ZrO_2 was judged to be by far the most reactive, whereas CeO_2 - ZrO_2 and Y_2O_3 - ZrO_2 were judged to perform moderately well (in terms of the TBC not spalling). All showed chemical reactivity, however, with MgO forming large amounts of $MgSO_4$, and CeO_2 and Y_2O_3 each forming vanadates, although with some sulfate. The formation of cerium vanadate ($CeVO_4$) was somewhat unexpected, since CeO_2 shows some resistance to V_2O_6 reaction (see below), but this may have resulted because of the relatively high concentrations of vanadium and sulfur used.

THERMOCHEMISTRY OF VANADATE-SULFATE MELTS: REVIEW AND DISCUSSION

The principal driving force for the degradation of TBCs by hot corrosion is chemical reaction between the stabilizing oxides (e.g., Y_2O_3 , CeO_2 , etc.) and the molten vanadate-sulfate engine deposits, or essentially vanadate-sulfate melts. Vanadium-containing melts of relatively low V_2O_6 activity (e.g., $NaVO_3$) can cause phase reversion in CeO_2 - ZrO_2 TBCs (and possibly In_2O_3 - ZrO_2 TBCs) by a "mineralization" effect where no chemical reaction of the CeO_2 can be detected (13). However, this is of second magnitude compared to hot corrosion chemical reaction. The thermochemistry of the vanadate-sulfate melt determines whether chemical reaction, or corrosion, of the TBC components will occur, and it is thus the ultimate factor in deciding TBC life in corrosive environments.

Mechanism of Vanadate Hot Corrosion of Y_2O_3 - ZrO_2 TBCs

As established in DOE-sponsored research (9), and since verified by others, the attack of vanadium on yttria-stabilized zirconia (YSZ) thermal barrier coatings occurs by:



where Y_2O_3 in solid solution in the ZrO_2 matrix reacts with the V_2O_6 (l) component of the vanadate-sulfate engine deposit to produce highly stable, solid YVO_4 (mp 1810°C) and solid ZrO_2 , but with the ZrO_2 being destabilized and in the monoclinic phase structure. No chemical reaction of V_2O_6 with ZrO_2 is normally detected. Reaction [1] can be confirmed by heating thin deposits of $NaVO_3$ on sintered YSZ pellets, where one then sees masses of acicular YVO_4 crystals formed on the YSZ surface by outward diffusion of Y_2O_3 , while destabilized monoclinic ZrO_2 is left below (14). Specific details of the crystallographic orientation of YVO_4 growing on YSZ have been revealed by thin film TEM (15), while the diffusion of V_2O_6 and Y_2O_3 within YSZ has been studied by Rutherford back-scattering (16).

The activity of V_2O_6 (l) determines whether reaction [1] will occur, since YVO_4 and ZrO_2 are pure solids (activity = 1), and although Y_2O_3 is in solid solution in ZrO_2 (act. < 1), its activity is fixed until reaction [1] actually commences. It is important therefore to know the V_2O_6 activity in vanadate-

sulfate engine deposits to predict when reaction [1] is possible, and to evaluate alternative stabilizers for improving the hot corrosion resistance of TBCs. As an example, the activity coefficient (γ) for 0.045 mol-fraction (8-wt%) of Y_2O_3 in ZrO_2 at 2500°C has been measured as ~0.1 (17), and is probably lower at 800-900°C (assume 0.01), since negative deviation from ideal solution behavior normally increases with decreasing temperature. Using the assumed $\gamma(\text{V}_2\text{O}_6)$ of 0.01, one can obtain an approximation of the act.(V_2O_6) at which reaction [1] should commence by thermodynamic calculation using Gibbs energy data provided by Yokokawa et al (18), viz.,

$$\Delta G^\circ_{800\text{C}} = \sum \Delta_f G^\circ_{\text{products}} - \sum \Delta_f G^\circ_{\text{reagents}} = -RT \ln K \quad [2]$$

$$K = \frac{(\text{act. YVO}_4)^2 \times (\text{act. ZrO}_2)}{(\text{act. V}_2\text{O}_6) \times (\text{act. Y}_2\text{O}_3)} = 1.803 \times 10^{11} = \frac{1}{(4.5 \times 10^{-4}) \times (\text{act. V}_2\text{O}_6)}$$

or, therefore $\text{act.}(\text{V}_2\text{O}_6) \geq 1.2 \times 10^{-8}$ for reaction [1] to occur

This value of $\text{act.}(\text{V}_2\text{O}_6)$ is exceeded by the $\text{act.}(\text{V}_2\text{O}_6)$ of $\sim 10^{-4}$ found for NaVO_3 at 850°C (see below), and therefore it is consistent that YSZ reacts readily with molten NaVO_3 ($\text{Na}_2\text{O} \cdot \text{V}_2\text{O}_6$), but not with the more basic Na_3VO_4 ($3\text{Na}_2\text{O} \cdot \text{V}_2\text{O}_6$), as found in the next section.

Lewis Acid/Base Reaction of Ceramic Oxides with Sodium Vanadates

Fig. 2 shows the reaction behavior of a number of oxides of increasing acidity as these are heated at 700-900°C with vanadium compounds of increasing acidity; i.e., Na_3VO_4 ($3\text{Na}_2\text{O} \cdot \text{V}_2\text{O}_6$), NaVO_3 ($\text{Na}_2\text{O} \cdot \text{V}_2\text{O}_6$), and pure V_2O_6 (19). Two important aspects of Fig. 2 should be noted. First, the reactions are primarily controlled by the Lewis acid/base nature of the oxide, with no reaction occurring when the Lewis basicities are approximately equal. A compound such as NaVO_3 can react as an acid, providing V_2O_6 , with an oxide of the basicity of Y_2O_3 , but as a base, providing Na_2O , with oxides of the acidity of GeO_2 or Ta_2O_5 .

Second, the ceramic oxides react with either the Na_2O or V_2O_6 component of the sodium vanadate compounds, and not with the compounds themselves. The role of the sodium vanadate compound is only to make Na_2O or V_2O_6 available at some certain level of activity. The reaction products consist of multiples of Na_2O or V_2O_6 with the various oxides, as for example, $2\text{Na}_2\text{O} \cdot 9\text{GeO}_2$, $\text{Na}_2\text{O} \cdot 2\text{Ta}_2\text{O}_5$, $\text{Y}_2\text{O}_3 \cdot \text{V}_2\text{O}_6$ (i.e., 2YVO_4), etc. An exception to this rule was found in later experiments with Sc_2O_3 , which reacts with NaVO_3 to form $3\text{NaVO}_3 \cdot \text{Sc}_2\text{O}_3$ at temperatures below 880°C (20). The oxidation state of the different cations does not change, except for the case of CeO_2 where Ce^{4+} goes to Ce^{3+} during the formation of CeVO_4 (see below).

INCREASING ACIDITY →			
	<u>Na_3VO_4</u>	<u>NaVO_3</u>	<u>V_2O_5</u>
<u>Y_2O_3</u>	NR	YVO_4	YVO_4
<u>CeO_2</u>	NR	NR	CeVO_4
<u>ZrO_2</u>	NR	NR	ZrV_2O_7 (BUT SLOWLY)
<u>GeO_2</u>	$\text{Na}_4\text{Ge}_9\text{O}_{20}$	$\text{Na}_4\text{Ge}_9\text{O}_{20}$ ^(*)	NR
<u>Ta_2O_5</u>	NaTaO_3	$\text{Na}_2\text{Ta}_4\text{O}_{11}$	$\alpha\text{-TaVO}_5$

NR = NO REACTION
(*) AS PPT FROM H_2O SOLN

Fig. 2 Lewis acid/base reaction of selected oxides with sodium vanadates and V_2O_6 .

Previous Studies of Vanadate-Sulfate Thermochemistry

Although numerous publications on vanadate-sulfate hot corrosion can be found in the literature, only four pertain to the actual thermochemistry of vanadate-sulfate deposits. These are listed in Table 1.

TABLE 1

Past Studies of the Thermochemistry of Vanadate-Sulfate Melts

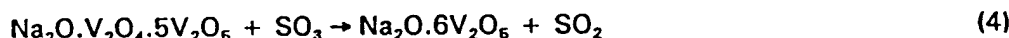
<u>Year</u>	<u>Authors/Reference</u>	<u>Topic/Conclusions</u>
1982	Luthra & Spacil, Ref. 21	Thermodynamic calculation of Na,V,S deposition in gas turbines; found $\gamma(V_2O_6)$ of 0.18 and 0.08 at 750° and 900°C for Na/V = 2 and 8.7×10^{-4} and 3.6×10^{-4} p(SO ₃), resp.
1984	Mittal & Elliott, Ref. 22	Electrochemical study of Na ₂ O-V ₂ O ₆ melts, with Na ₂ O activity by electrode EMF, V ₂ O ₆ activity by Gibbs-Duhem integration; melts found to be highly nonideal
1989	Hwang & Rapp, Ref. 23	Calculation of Na ₃ VO ₄ , NaVO ₃ and V ₂ O ₆ concentrations in melts; vanadate-sulfate melts assumed to be ideal; predicted ~20% V ⁴⁺ in Na-V melts at 900°C and -log Na ₂ O of 15.3~18.7
1995	Reidy & Jones, Ref. 24	TGA study of SO ₃ equilibrium with NaVO ₃ at 800°C, and reaction of melt with CeO ₂ ; for lowest V ₂ O ₆ levels, found $\gamma(V_2O_6) \approx 0.01$

Question of V⁴⁺/V⁶⁺ in Vanadate-Sulfate Melts

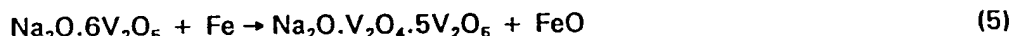
In the older boiler corrosion research (1), it was postulated by many that vanadium-rich deposits contained V⁴⁺/V⁶⁺ couples which transported oxygen by reactions of the type:



where one could have



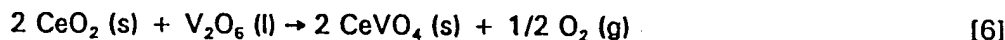
which might then be followed by



One solution proposed for vanadate-induced corrosion by heavy oils in boilers was the use of "low excess air", or LEA. In pilot boiler tests (25) using low-quality oil containing 2.57 wt% S, 53 ppm Na, and 350 ppm V, the vanadium in boiler-tube deposits forming at 1300°F (704°C) was 91% V₂O₆, 9% V₂O₃ and/or V₂O₄ with 15% excess air, but only 24% V₂O₆ with 76% V₂O₃ and/or V₂O₄ at 1% excess air. In the latter instance, there was significantly lower deposit formation and boiler-tube corrosion, presumably because of the higher melting points and physical nature of V₂O₃ and V₂O₄. These data therefore indicate that V₂O₃ or V₂O₄ can be found in boiler deposits. However, this occurs under nearly reducing combustion conditions, and also where there is the possibility of V₂O₆ reduction by tube metal oxidation (the 1300°F tube deposits in fact consisted of about 75% corrosion product).

Whether V^{4+} would occur in significant amounts in vanadate-sulfate melts on TBCs in gas turbines operating at high air/fuel ratios, or in laboratory studies of vanadate-sulfate melts under ambient O_2 partial pressures, is another question. In these cases, the conditions are oxidizing, and the ceramic oxides involved (ZrO_2 , Y_2O_3 , etc.) are stable to very low $p(O_2)$, except for CeO_2 which, as the pure oxide at 1000°C, begins to be reduced to $CeO_{1.83}$ at $\sim 10^{-12}$ atm of O_2 . Calculations by Hwang and Rapp (23) indicate that Na_2SO_4 -30 mol% $NaVO_3$ melts at 900°C and ambient $p(O_2)$ should contain $\sim 20\%$ V^{4+} over the log act.(Na_2O) range of -15.3 to -18.7. However, this contradicts the findings of Mittal and Elliott (22) who conclude that vanadium in liquid Na_2O - V_2O_6 exists only as V^{6+} over the measured log act.(Na_2O) range of -13 to -20 at 852°C (see below). They support their conclusion by citing Block-Bolton and Sadoway (26) who found no V^{4+} in liquid V_2O_6 at 1200K (927°C) for $p(O_2) > 0.06$ atm. Also, it appears that Na_2O stabilizes V^{6+} in V_2O_6 , as proposed by Mittelstadt and Schwerdtfeger (27) who observed that whereas Na_2O - $0.5V_2O_6$ begins to reduce to V^{4+} at 10^{-2} atm $p(O_2)$ at 1000°C, Na_2O - V_2O_6 is stable down to 10^{-6} atm $p(O_2)$.

As another consideration, when CeO_2 reacts with the V_2O_6 component of vanadate-sulfate melts (see below), the reaction goes as,



A reduction occurs in reaction [6], but one can not be certain, a priori, whether it is the cerium cation (4^+ to 3^+) or the vanadium cation (5^+ to 4^+) that is reduced. To answer this question, Reidy and Swider (28) examined $CeVO_4$ by X-ray absorption spectroscopy (XAS) and showed that cerium is in the Ce^{3+} state in $CeVO_4$, and vanadium thus in the V^{6+} state. Taken overall, the literature data indicate that, for the oxidizing conditions postulated, V^{4+} is unlikely to be significant in the thermochemistry of vanadate-sulfate melts relating to TBC ceramic hot corrosion.

Thermodynamic Modeling of Acid-Base Melts

The activity of a component of a solution or melt is defined according to

$$\text{act.} = \gamma \times X \quad [7]$$

where act. is the component activity, γ is the activity coefficient, and X is the mol-fraction of the component. For ideal solutions, the activity coefficient is unity, and the activity of a component is simply equal to its mol-fraction. Almost all melt solutions are nonideal, however, and in that case, γ changes with the overall composition of the solution. To describe how γ varies with melt composition, solution scientists often adopt "solution models" which, following theoretical or empirical reasoning, are intended to predict the dependence of γ on melt composition.

Many solution models have been developed since, in different types of melts, the melt components interact in different ways, which must be taken into account. For oxide systems which involve strong acid-base chemical interactions (such as at present), the best model appears to be the Ideal Mixing of Complex Components (IMCC) model developed by Bonnell and Hastie (29). This model is capable of describing the very large changes in the ratio of formal concentration to thermodynamic activity (10^{10} or more) that can occur in strong acid-base reactions, as demonstrated by Bonnell and Hastie for complex slags containing such components as Na_2O , SiO_2 , K_2O , and Al_2O_3 .

The IMCC model uses Gibbs-energy-minimization by computer to determine the "free" mol-fraction, as opposed to the nominal mol-fraction, of a component such as K_2O , when that component exists in the melt in competing equilibria with other components by reactions such as,





[9]



[10]

It is thus akin to the NASA-developed computer calculation of the equilibria of molecular species in high temperature gases, and also to the calculations made for the $Na_2O-V_2O_6-SO_3$ system by Luthra and Spacil (21). The IMCC model assumes ideal mixing of the various "product molecules" once they have been formed by the chemical reactions indicated; that is, there is assumed to be no other type of interaction between the product molecules, after they are formed, that would yield significant additional Gibbs energy of solution for the melt.

This raises the question of whether such "product molecules" actually exist in melts. For gases, techniques such as high temperature mass spectrometry, infrared spectroscopy or gas chromatography can be used to identify gas phase molecules, and, if conditions are such that kinetics do not interfere, the thermodynamically-predicted gaseous species generally are found, and in the approximate quantities calculated. With melts, however, it is not possible to make an equivalent molecular identification of melt species. About the best information available is obtained with binary metal melts such as Sb-Mg, where plotting the excess solution stability (d^2G^E/dx_i^2 , where G^E is the excess integral molar free energy of a solution) against melt composition may reveal peaks at certain stoichiometries which indicate the formation of melt complexes such as Mg_3Sb_2 (30). Bonnell and Hastie (29) approach this problem by considering that "-- the liquid components are not necessarily independent molecular or ionic species, but serve to represent the local associative order." The goodness of fit between solution model prediction and experimental results obtained by Bonnell and Hastie appears to justify their hypothesis, although it remains difficult to envision the arrangement of atoms in the melt that this would imply.

For the purposes of the present Report, the discussion in this section has mostly only philosophical implications, since no solution model for the $Na_2O-V_2O_6-SO_3$ system is proposed from our NRL research. The NRL results do contain, however, substantial experimental data (see below) that could be used in the development of such a solution model.

Study of $Na_2O-V_2O_6$ Melts by Mittal and Elliott

Mittal and Elliott (22) consider sodium vanadate deposits to be mixtures of vanadium oxide (V_2O_5) and sodium oxide (Na_2O) produced by oxidation of Na,V-impurities in fuel during combustion. Our NRL research has taken the same approach, but with the effect of engine gas SO_3 added in. Since the Mittal and Elliott paper in some ways represents the "starting point" for our NRL work, their paper will be discussed in detail here.

Mittal and Elliott made electrochemical measurements at 757-937°C of the activity of Na_2O in melts having a V_2O_5 mol-fraction range of 0.5 to 0.9; that is, totally molten mixes from $Na_2O.V_2O_5$ (i.e., $NaVO_3$) up to $Na_2O.9V_2O_5$ in the V_2O_5 -rich half of the $Na_2O-V_2O_5$ phase diagram (Fig. 3). These composition and temperature

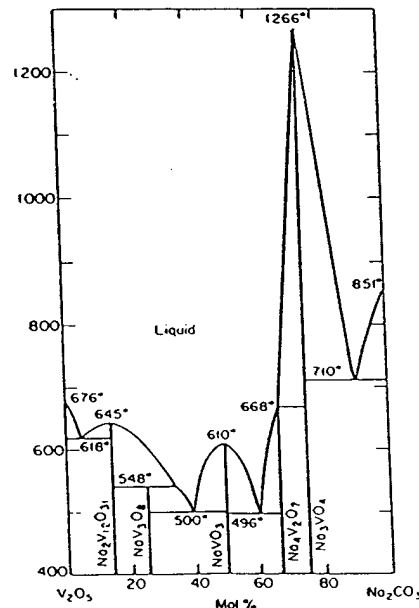
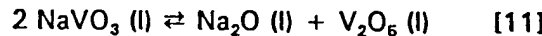


Fig. 3 Phase diagram for $V_2O_5-Na_2CO_3$ (Na_2O). Ref. 31.

ranges are generally thought to be among the most corrosive in terms of vanadate hot corrosion. The corresponding activities for V_2O_6 were calculated by integration of the Gibbs-Duhem equation.

The activities of Na_2O and V_2O_6 found by Mittal and Elliott for molten $Na_2O-V_2O_6$ mixes at 852°C (1125K) are plotted in Fig. 4. At 0.5 mol-fraction of V_2O_6 (that is, for $Na_2O.V_2O_6$ or $NaVO_3$), the log of Na_2O activity is -13.13, and that of V_2O_6 is -3.62, giving a log activity product of -16.75. This value can be compared with thermodynamic calculation for the reaction,



where the log activity product of Na_2O and V_2O_6 is found to be -16.93, using thermodynamic data by Yokokawa et al (18) and Barin (32). This is good agreement which supports the Mittal and Elliott results as being correct.

The data of Mittal and Elliott are plotted in Fig. 5 with Na_2O and V_2O_6 as the melt components. This plotting shows V_2O_6 to have a strong negative deviation from ideal solution behavior. The V_2O_6 activity coefficient for $X(V_2O_6) = 0.5$ (i.e., in molten $NaVO_3$) is $\sim 4.8 \times 10^{-4}$, as obtained by dividing the V_2O_6 activity, log -3.62, by the V_2O_6 mol-fraction concentration, 0.5. The Mittal and Elliott data can also be recalculated and plotted to reflect $NaVO_3$ and V_2O_6 as being the melt components. This yields Fig. 6, where V_2O_6 continues to exhibit a negative deviation from ideal solution behavior. Fig. 6 indicates therefore that $NaVO_3$ and V_2O_6 do not mix in a totally ideal fashion, as assumed in the calculations by Hwang and Rapp (23). As a final

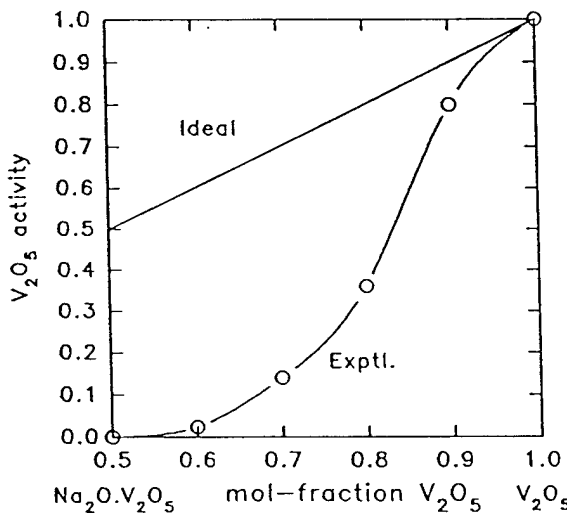


Fig. 5 Solution behavior of $Na_2O-V_2O_6$ at 852°C, taking Na_2O and V_2O_6 as the melt components.

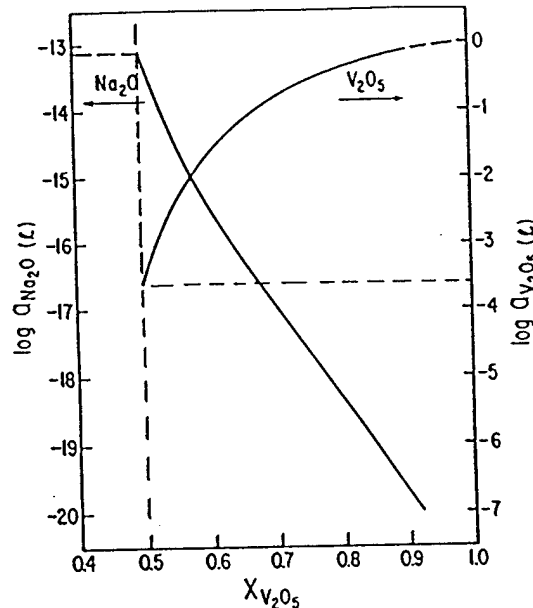


Fig. 4 Log act.(Na_2O) and log act.(V_2O_6) in the $Na_2O-V_2O_6$ binary system at 1125 K (852°C). From Ref. 22.

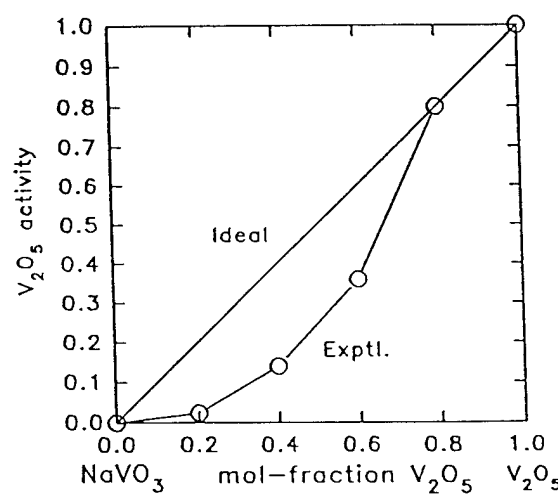
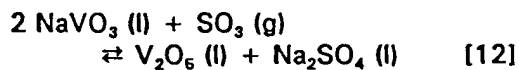


Fig. 6 Solution behavior of $Na_2O-V_2O_6$ at 852°C, with $NaVO_3$ and V_2O_6 as the melt components.

side point, notice that there are no obvious inflections in the experimental log act.(Na₂O) curve of Mittal and Elliott (Fig. 4) such as might reflect any influence in the melt behavior resulting from the compounds, Na₂O·3V₂O₆ (NaV₃O₈) and Na₂O·6V₂O₆ (Na₂V₁₂O₃₁), which occur within the Na₂O-V₂O₆ composition range studied (Fig. 3).

Thermogravimetric Equilibrium of SO₃ with NaVO₃ Melts

The mutual interaction between Na₂O, V₂O₆ and SO₃, as occurs in engine vanadate-sulfate deposits, was investigated by a thermogravimetric technique in which SO₃ at increasing partial pressures was equilibrated with molten NaVO₃ at 800°C. The reaction is described by,



Reaction [12] was identified by Luthra and Spacil (21) as being the major reaction in determining the composition of vanadate-sulfate engine deposits under marine gas turbine conditions. Also, we have shown earlier that whereas CeO₂ does not react chemically with pure molten NaVO₃, an overpressure of SO₃ yields V₂O₆ by reaction [12], with CeVO₄, then forming by reaction between CeO₂ and V₂O₆ (19). Note that one starts with pure NaVO₃ in reaction [12] and then essentially adds, by using initially very low partial pressures of SO₃, small increments of V₂O₆ and Na₂SO₄ to the original NaVO₃. The thermochemical behavior of the resultant melts would therefore be expected to show a smooth transition from the thermochemical properties found by Mittal and Luthra for 0.5 mol-fraction Na₂O-V₂O₆ (NaVO₃), at least for the initial low V₂O₆- and Na₂SO₄-content mixes.

Our thermogravimetric analysis (TGA) furnace system used a two-stage gas dilution arrangement which employed electronic mass flow gas controllers to give SO₂ partial pressures of down to 10⁻⁸ bar in the furnace input air (33). The SO₂/air input mixture was equilibrated over Pt at temperature in the furnace (Fig. 7), with the SO₃-SO₂-air mixture then passing over the NaVO₃ melt (50 mg) which was contained in a shallow, balance-suspended Pt planchet. After an initial weight loss of ~2% (the NaVO₃ contained about 2% water), the system showed negligible weight change (< 0.2 mg) for periods in excess of 50 hrs under slowly flowing (50 ml/min) air dried over Drierite™.

Attainment of SO₃ equilibrium. As the p(SO₃) was lowered, the time required to reach equilibrium became progressively longer, so that for p(SO₃) ≤ 10⁻⁶, 100 hrs or more would be needed for equilibrium by simple exposure to the test p(SO₃). Our procedure therefore was to bring the NaVO₃ to both above and below equilibrium weight (in separate measurements) at a higher p(SO₃), and then return the system to the test p(SO₃) and monitor the wgt gain vs. time slopes (positive or negative), which were back-extrapolated to identify the true equilibrium weight (33). The time for equilibrium also was found to be proportional to the weight of NaVO₃, taking approximately twice as long for 100 mg as 50 mg NaVO₃. This experience raises the question, at least in the author's mind, of how massive amounts of melt (up to 25 gms) in a narrow electrochemical cell could become equilibrated with low p(SO₃)'s (≤ 10⁻⁴ atm) in a reasonable time. Two possible answers come to mind: first, many

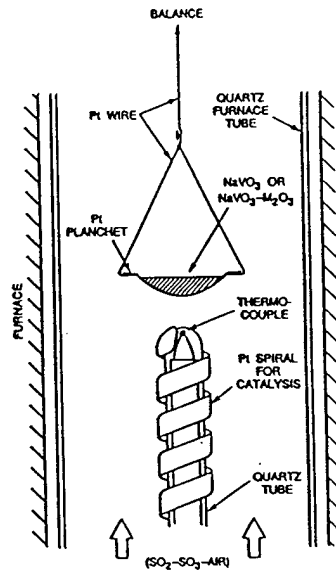


Fig. 7 Arrangement of specimen melt planchet (Pt) within furnace.

of the electrochemical experiments were at 900°C rather than 800°C as here, and the 100°C higher temperature may significantly speed up SO₃ diffusion; second, our melt is, at least initially, pure NaVO₃, whereas most electrochemical experiments involving SO₃ equilibrium use melts consisting mostly of sulfates, and it may be that SO₃, perhaps as S₂O₇⁻, diffuses more rapidly through sulfate-based melts than vanadate-based melts.

Thermodynamic Analysis of SO₃-NaVO₃ Equilibrium Data

The equilibrium weight gain data for 50 mg (0.41 mmols) of dried NaVO₃ under different p(SO₃) at 800°C are presented in Fig. 8. The weight gain behavior was reversible and reproducible (to within ± 0.2 mg), which confirms that SO₃ is absorbed, or given off, without any permanent change in the NaVO₃ melt. Conversion of the NaVO₃ completely to Na₂SO₄ and V₂O₆ by reaction [12] would yield an equilibrium weight gain of 16.4 mg.

From the weight gain and stoichiometry of reaction [12], one can calculate the mol-fraction of V₂O₆ experimentally formed at each p(SO₃), as listed in Table 2. And, since the activity coefficient equals unity for ideal solutions and therefore act. = X, the "ideal" mol-fraction can be calculated from thermodynamic data following the procedure outlined in reaction [2]. Using the thermodynamic data provided by Luthra and Spacil (21) for the reagents and products in reaction [12], one obtains,

$$K = 91.61166 = \frac{\text{act.}(V_2O_6) \times \text{act.}(Na_2SO_4)}{\text{act.}(NaVO_3)^2 \times p(SO_3)} \quad [13]$$

which, by transposing p(SO₃) and setting act. = X, reduces to a quadratic equation in the unknown, x, that can be solved by numerical approximation on the computer for each p(SO₃),

$$91.61166 \times p(SO_3) = \frac{x^2}{(1-2x)^2} \quad [14]$$

The "ideal" mol-fractions (or "ideal" activities) for V₂O₆ so obtained are listed in Table 2. Division of the ideal V₂O₆ mol-fraction by the experimental V₂O₆ mol-fraction then yields an approximate $\gamma(V_2O_6)$, listed in Table 2 as " $\gamma(V_2O_6)$ -Approx. 1" for each p(SO₃), or alternatively, for each melt composition.

However, approximation 1 for $\gamma(V_2O_6)$ is not correct since the actual value for act.(V₂O₆) has not been determined. Approximation 1 treats NaVO₃, Na₂SO₄ and V₂O₆ as all behaving ideally, which is almost certainly not true. Luthra and Spacil (21), for example, considered NaVO₃ and Na₂SO₄ to be ideal, but V₂O₆ to be nonideal because of its stronger interactions with the melt. If V₂O₆ is assumed nonideal, while NaVO₃ and Na₂SO₄ are ideal, then equation [14] can be modified to give, using the experimentally-determined mol-fractions, a second approximation for $\gamma(V_2O_6)$ according to,

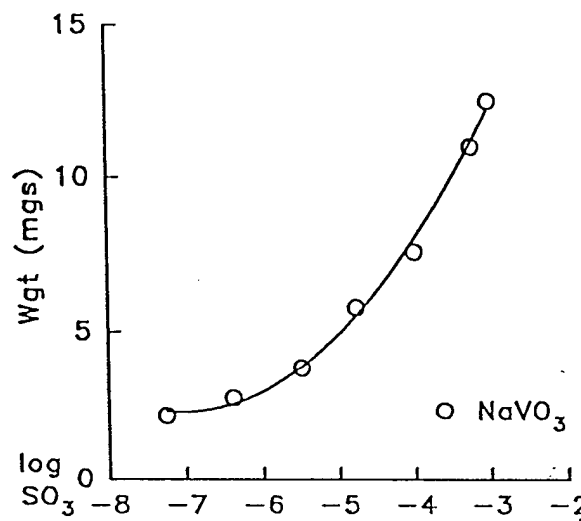


Fig. 8 Weight gain behavior of NaVO₃ equilibrated at 800°C with the indicated SO₃ partial pressures.

$$\gamma(V_2O_6)\text{-Approx. 2} = \frac{91.61166 \times p(SO_3) \times X(NaVO_3)^2}{X(Na_2SO_4) \times X(V_2O_6)} \quad [15]$$

The values for $\gamma(V_2O_6)$ -Approx. 2 are listed in Table 2, with both approximations being plotted in Fig. 9. Inspection of Fig. 9 suggests that $\gamma(V_2O_6)$ -1 is probably closer to correct at the higher $p(SO_3)$, while $\gamma(V_2O_6)$ -2 is more nearly correct at the lower $p(SO_3)$ values. This may be partially explained along the following lines. Note in equation [13] that at the lowest $p(SO_3)$, $NaVO_3$ is almost pure, and its activity thus essentially 1. Under these circumstances, $K \times p(SO_3)$, a known value, becomes equal to the activity product, i.e., $act.(V_2O_6) \times act.(Na_2SO_4)$. Determining $act.(V_2O_6)$ is then a matter of correctly apportioning the activity product. In Approx. 1, all species are treated as ideal, and $act.(V_2O_6) = act.(Na_2SO_4)$, with $act.(V_2O_6)$ being therefore simply 1/2 of the activity product. In Approx. 2, where Na_2SO_4 (II) but not V_2O_6 (II) is assumed ideal, $act.(Na_2SO_4) = X(Na_2SO_4)$, and division of the activity product by $X(Na_2SO_4)$ from Table 2 yields a lower activity for the "nonideal" V_2O_6 Species. In actuality, Na_2SO_4 (II) is probably not totally ideal, and $act.(V_2O_6)$ should fall somewhere between the Approx. 1 and Approx. 2 values. One might expect also that, as their mol-fraction concentration increases at high $p(SO_3)$, V_2O_6 and Na_2SO_4 would exhibit activity coefficients closer to unity (cf. Fig. 5), making Approx. 1 more nearly correct. Therefore, for purposes of a later comparison (see below), an averaged $\gamma(V_2O_6)$ was calculated, which is shown as $\gamma(V_2O_6)$ -Avg in Fig. 9. The calculated average is weighed toward $\gamma(V_2O_6)$ -2 at the lower $p(SO_3)$, and $\gamma(V_2O_6)$ -1 at the higher $p(SO_3)$.

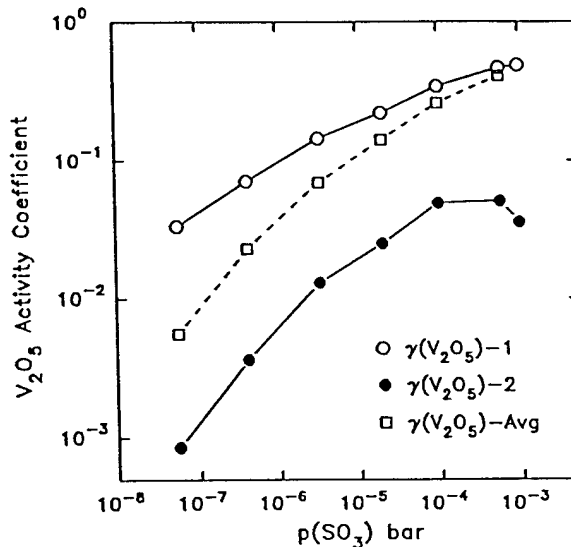


Fig. 9 Values for $\gamma(V_2O_6)$, Approxs. 1 and 2, and $\gamma(V_2O_6)$ -Avg. plotted against $p(SO_3)$.

TABLE 2

Experimental Results and Calculated Approximations
for $\gamma(V_2O_6)$ in $NaVO_3$ Equilibrated with SO_3 at 800°C

$p(SO_3)$ in bar	Wgt. gain in mg	Exptl. $X(V_2O_6)$	"Ideal" $X(V_2O_6)$	$\gamma(V_2O_6)$ - Approx. 1	$\gamma(V_2O_6)$ - Approx. 2	$\gamma(V_2O_6)$ - Avg.
5.6×10^{-8}	2.2	0.0670	0.00225	0.0336	8.6×10^{-4}	0.0055
4.1×10^{-7}	2.8	0.0853	0.00603	0.0707	3.6×10^{-3}	0.023
3.3×10^{-6}	3.8	0.116	0.0167	0.144	1.3×10^{-2}	0.069
2.0×10^{-5}	5.8	0.177	0.0392	0.221	2.5×10^{-2}	0.14
1.0×10^{-4}	7.6	0.232	0.0799	0.344	4.9×10^{-2}	0.26
5.8×10^{-4}	11.0	0.335	0.157	0.469	5.1×10^{-2}	0.41
9.9×10^{-4}	12.5	0.381	0.186	0.488	3.6×10^{-2}	0.49

Note that the $\gamma(V_2O_6)$ values in Table 2 depend, of course, upon the thermochemical data selected. If data incorporating values provided more recently by Yokokawa et al (18) are used, the value of K is raised from 91.61166 to 168.8 which, for example at $p(SO_3) = 5.6 \times 10^{-8}$ bar, changes $\gamma(V_2O_6)$ -Approx. 2 for from 8.6×10^{-4} to 1.6×10^{-3} .

Reaction of Candidate Stabilizing Oxides with SO₃-NaVO₃

The equilibrated SO₃-NaVO₃ TGA technique was used to investigate the reaction of MgO, Y₂O₃, Sc₂O₃ and In₂O₃ (33), Cr₂O₃ and SnO₂ (34), and CeO₂ (24) with the Na₂O-V₂O₆-SO₃ melt system, with the mix ratio of 0.41 mmols NaVO₃ and 0.1 mmols of oxide normally being employed. As summarized in Fig. 10a-10g, the results serve to rank the potential vanadate-sulfate hot corrosion resistance of candidate stabilizing oxides for ZrO₂. They also provide information about the nature of the different reactions that the various oxides undergo with vanadate-sulfate melts. These can be broken down into categories as described below:

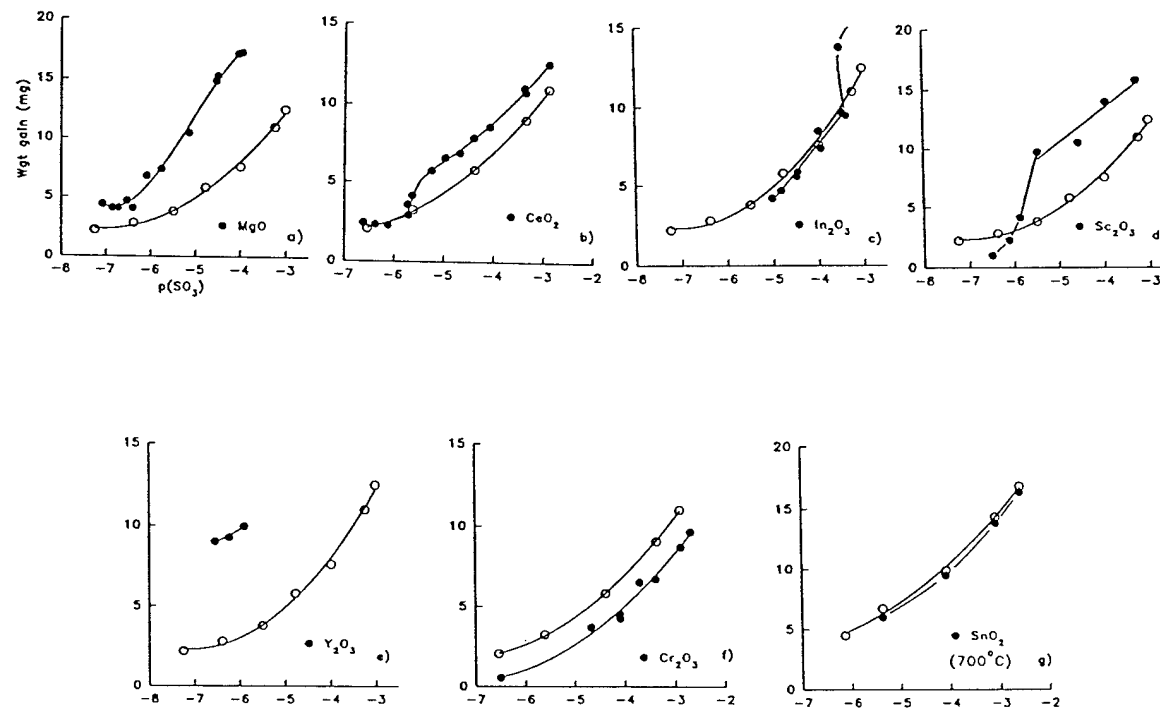


Fig. 10 (a-g) Weight gain vs. $p(SO_3)$ at 800°C for NaVO₃ (0.41 mmols) plus various candidate ZrO₂-stabilizing oxides (0.10 mmols).

Formation of soluble product. This is exemplified by MgO (Fig. 10a), where even at a $p(SO_3)$ of 10^{-7} bar, the MgO-NaVO₃ mix shows a higher weight gain than for pure NaVO₃, even though the amount of NaVO₃ is the same in each case. The additional weight gain must come from the uptake of SO₃ by either MgO or Na₂O, since vanadyl sulfate is ruled out at such low $p(SO_3)$. Low melting mixtures of V₂O₆-(2MgO.Na₂O) or V₂O₆-(MgO.Na₂O) can form (35), but these would yield no change in weight. Also, thermodynamic calculations indicate that the displacement of Na₂O by MgO by, e.g.,

$\text{MgO} + \text{Na}_2\text{O} \cdot \text{V}_2\text{O}_6 \rightarrow \text{Na}_2\text{O} + \text{MgO} \cdot \text{V}_2\text{O}_6$, is highly unfavored. Solid MgSO_4 also appears not to be possible, since a critical $p(\text{SO}_3)$ of 1.6×10^{-6} bar is indicated for $\text{MgO}(\text{s}) + \text{SO}_3 \rightarrow \text{MgSO}_4(\text{s})$ at 800°C . However, if soluble MgSO_4 is formed, then appreciable MgSO_4 could be produced even at $p(\text{SO}_3) \sim 10^{-7}$ bar. Moreover, since such a system would have two degrees of freedom by the phase rule, some MgSO_4 (II) can be formed no matter how low the $p(\text{SO}_3)$; i.e., there will be no one critical $p(\text{SO}_3)$ for onset of reaction. The hypothesis of a soluble MgSO_4 product is consistent also with the MgO-ZrO_2 TBC burner rig tests (12) burning Na,V,S-containing fuel, where major amounts of MgSO_4 but only minor amounts of Mg vanadate were found on the TBC surface. At the higher $p(\text{SO}_3)$ values in Fig. 10a, there is an upturn in weight gain which presumably reflects the onset of magnesium vanadate formation, since the reaction, $2\text{MgO} + \text{V}_2\text{O}_6 = 2\text{MgO} \cdot \text{V}_2\text{O}_6$ is thermodynamically predicted to be possible at 800°C at $\text{act.}(\text{V}_2\text{O}_6) = 8 \times 10^{-6}$ bar. This could not be confirmed unequivocally by x-ray diffraction, however, which in this case gave complex and diffuse patterns (common for Na/Mg vanadate-sulfate phases from melts). Nonetheless, taken overall, the weight gain behavior in Fig. 10a indicates that melt-soluble MgSO_4 is formed at low $p(\text{SO}_3)$ in the $\text{MgO-NaVO}_3-\text{SO}_3$ system, but that Mg vanadate may be produced at high $p(\text{SO}_3)$ (i.e., at high V_2O_6 melt activities).

Metal vanadate formation once critical V_2O_6 activity reached. This behavior is shown by CeO_2 (Fig. 10b), In_2O_3 (Fig. 10c), and Sc_2O_3 (Fig. 10d), although the case for Sc_2O_3 is complicated by the occurrence of $3\text{NaVO}_3 \cdot \text{Sc}_2\text{O}_3$. With CeO_2 and In_2O_3 , the weight gain curve is just the same as pure NaVO_3 (in other words, the oxide is as chemically inert as the Pt planchet itself) up to a critical $p(\text{SO}_3)$, where the melt V_2O_6 activity is raised (via reaction 12) sufficiently that the oxide begins to react with V_2O_6 to form the vanadate. The weight gain for CeO_2 and In_2O_3 is then almost vertical, reflecting the insolubility of the vanadate product. Since the rare earth oxides and their vanadates are high-melting compounds with excellent x-ray diffraction patterns, one can show by x-ray, as for CeO_2 and CeVO_4 (see below), that only oxide exists below, and only vanadate above, the critical $p(\text{SO}_3)$, or actually V_2O_6 activity.

With Sc_2O_3 , the weight gain curve for $\text{Sc}_2\text{O}_3\text{-NaVO}_3$ is below that of NaVO_3 up to the critical $p(\text{SO}_3)$. Although not originally understood (32), this behavior results because, at temperatures below 880°C (20), Sc_2O_3 reacts with NaVO_3 to give the weak compound, $3\text{NaVO}_3 \cdot \text{Sc}_2\text{O}_3$. This compound reduces the activity of Na_2O , and therefore less SO_3 is taken up than with pure NaVO_3 of equivalent weight. The weight gain rise leans somewhat from the vertical in this case, which possibly reflects the "breaking" of the $3\text{NaVO}_3 \cdot \text{Sc}_2\text{O}_3$ compound as $p(\text{SO}_3)$ increases. Also, our initial X-ray analysis was in error, with ScVO_4 being correctly identified as the only scandium compound above the critical $p(\text{SO}_3)$, but Sc_2O_3 as the compound below, when in fact it was $3\text{NaVO}_3 \cdot \text{Sc}_2\text{O}_3$. The difficulty in distinguishing between Sc_2O_3 mixed with NaVO_3 and $3\text{NaVO}_3 \cdot \text{Sc}_2\text{O}_3$ arises because all of the strong peaks for Sc_2O_3 (x-ray standard pattern JCPDS 42-1463) are also contained in the $3\text{NaVO}_3 \cdot \text{Sc}_2\text{O}_3$ x-ray pattern (JCPDS 30-1241).

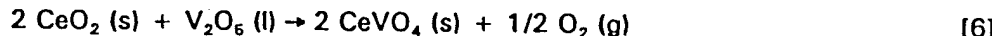
Direct reaction with pure NaVO_3 . In Fig. 10e, Y_2O_3 is sufficiently basic that it reacts directly with molten NaVO_3 to produce YVO_4 , which leaves the melt enriched in Na_2O . Therefore, when this system is equilibrated with even very low $p(\text{SO}_3)$, there is a high weight gain because of the pre-existing "reservoir" of Na_2O .

Another type of direct reaction occurs with Cr_2O_3 (Fig. 10f) which reacts with pure NaVO_3 and reduces the activity of Na_2O , probably by Na_2CrO_4 formation. This then yields less uptake of SO_3 than would be found with pure NaVO_3 alone, and over a wide $p(\text{SO}_3)$ range.

Inert to the $\text{NaVO}_3\text{-SO}_3$ system. Finally, SnO_2 (Fig. 10g) is chemically inert to the $\text{NaVO}_3\text{-SO}_3$ system, with the weight gain being essentially identical to that for NaVO_3 alone up to at least 1×10^{-3} bar of SO_3 . The resistance of SnO_2 to reaction with V_2O_6 may be one reason for its effectiveness in passivating fluid cracking catalysts against deactivation by vanadium impurities in crude oil (7).

Determining Act.(V₂O₆) without Assumption as to Act.(Na₂SO₄)

In calculating act.(V₂O₆) from the NaVO₃-SO₃ equilibrium weight gain data via equation [13], one is ultimately dealing with the activity product, act.(V₂O₆) × act.(Na₂SO₄), and an assumption concerning the Na₂SO₄ solution behavior (ideal or nonideal, and what activity coefficient?) must be made to obtain act.(V₂O₆). However, an alternative derivation of act.(V₂O₆), or more specifically, of $\gamma(V_2O_6)$, that is not dependent upon act.(Na₂SO₄) can be made on the basis of reaction [6],



In this case, CeO₂ and CeVO₄ are pure solids of low solubility (24), and p(O₂) is the atmospheric oxygen pressure of 0.21 bar so, at 800°C, the activity of V₂O₆(l) is fixed. Using the thermodynamic data for CeO₂(s), CeVO₄(s) and V₂O₆(l) provided by Yokokawa et al (18), the critical V₂O₆ activity necessary for reaction [6] can be calculated to be 6.2×10^{-4} .

The problem is to identify the V₂O₆ concentration at which reaction [6] just begins. This can be done by examination of Fig. 11, which shows that the weight gain step-up resulting from reaction [6] commences at a p(SO₃) of 3×10^{-6} bar, where the melt weight gain is 3.0 mg, corresponding to formation of 0.091 mol-fraction of V₂O₆ (and Na₂SO₄). If the theoretical V₂O₆ activity for Reaction [6] of 6.2×10^{-4} is divided by the experimental V₂O₆ mol-fraction of 0.091 from Fig. 11, a V₂O₆ activity coefficient of 7×10^{-3} results. This $\gamma(V_2O_6)$ agrees well with the $\gamma(V_2O_6)$ -Avg. of ~0.01 indicated in Fig. 9 for p(SO₃) = 4×10^{-7} bar, even though $\gamma(V_2O_6)$, in the present case, is determined on the basis of a different experimental reaction, and without regard to the Na₂SO₄ or NaVO₃ solution behavior.

As is well known, calculations such as above depend critically upon the accuracy of the thermodynamic data. Assuming an accumulated ± 10 kJ error in ΔG° for reaction [6] causes the derived $\gamma(V_2O_6)$ to vary from 2.1×10^{-2} to 2.2×10^{-3} . This error bar is shown for the datum point of $\gamma(V_2O_6) = 7 \times 10^{-3}$, X(V₂O₆) = 0.091 which has been included as representative of the present experiment for the $\gamma(V_2O_6)$ comparison in Fig. 14 below. It is not an insignificant error, but fits well within the data band. Good agreement is thus seen between two independent sets of experiments (i.e., SO₃-NaVO₃ equilibrium, and CeO₂ → CeVO₄ reaction), in which two different sets of thermodynamic data (Luthra & Spacil, and Yokokawa et al) were used. Error in the thermodynamic data is therefore unlikely to seriously invalidate the present results, especially in their role of serving to indicate the general range of V₂O₆ nonideality in vanadate-sulfate melts.

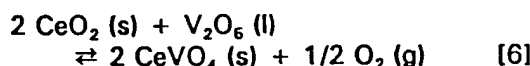
V₂O₆ Titration using CeVO₄ Formation as "Indicator" to Determine $\gamma(V_2O_6)$

Reaction [6] is analogous to the metallurgical reaction,



which has great significance in metallurgy. By reaction [16], one can, for a given temperature, determine either $\Delta_f G^\circ$ for MO, or the critical $p(O_2)$ for metal oxidation/reduction, provided that the other is known. Moreover, reaction [16] is totally independent of the gaseous environment. Large quantities of inert gases such as nitrogen or argon can be present, and there can be other reactions in which O_2 engages (e.g., $CO + 1/2 O_2 = CO_2$) but, if obeyed as written, reaction [16] will nonetheless remain independent.

For the case of reaction [6], a critical V_2O_6 (II) activity of 6.2×10^{-4} is required at 800°C, according to calculations based on the thermodynamic data of Yokokawa et al (18), for the reaction to proceed,



If obeyed as written, reaction [6] is independent of the melt composition, and the V_2O_6 (II) activity required for reaction [6] will always, at 800°C, be 6.2×10^{-4} regardless of melt composition. However, the V_2O_6 activity coefficient can, and most probably will, change with melt composition. Therefore, by finding the mol-fraction of V_2O_6 at which reaction [6] commences, one can potentially determine $\gamma(V_2O_6)$ for virtually any melt system in which an appropriate V_2O_6 activity for reaction [6] to proceed can be attained.

This idea was tested using melts consisting of 1 mmol of CeO_2 mixed with 4 mmol blends of vanadate-sulfate of four different compositions, viz., 100% $NaVO_3$, $NaVO_3$ -(10 mol%) Na_2SO_4 , $NaVO_3$ -(25 mol%) Na_2SO_4 , and $NaVO_3$ -(50 mol%) Na_2SO_4 . A series of varying amounts of V_2O_6 were added to the melt mixes, which were then heated at 800°C for 2 hrs in quiescent air and x-rayed to determine the amount of $CeVO_4$ formed. The relative amount of $CeVO_4$ produced was determined via the expression,

$$\% CeVO_4 = 100 \times \frac{[CeVO_4(200) \text{ Peak Hgt.}]}{[CeVO_4(200) \text{ Peak Hgt.}] + [CeO_2(111) \text{ Peak Hgt.}]} \quad [17]$$

which is an approximation of the integrated intensity ratio formulation commonly used to determine the relative amounts of crystal phases by x-ray diffraction (36). By extrapolation of the percent of $CeVO_4$ formation to zero (Fig. 13), one can ascertain the mmols of V_2O_6 that must be added to raise the melt V_2O_6 activity to the point at which $CeVO_4$ formation begins, and $CeO_2(s)$, $CeVO_4(s)$, $V_2O_6(II)$, and atmospheric O_2 are all in equilibrium; that is, when reaction [6] is obeyed.

The results yielded from Fig. 12 are tabulated in Table 3, where the calculated $\gamma(V_2O_6)$ is 6×10^{-3} for $NaVO_3$ -(10 mol%) Na_2SO_4 , to which 0.1031 X(V_2O_6) had been added. This X(V_2O_6) is near the 0.0853 X(V_2O_6) obtained by equilibrating $NaVO_3$ under 4.1×10^{-7} bar of SO_3 (cf. Table 2), and where $\gamma(V_2O_6)$ -Approx.2 was 3.6×10^{-3} . To obtain a better comparison, the data in Table 2 were linearly interpolated to 0.1031 X(V_2O_6), which yielded a value for $\gamma(V_2O_6)$ -Approx.2 of 9.1×10^{-3} . This latter $\gamma(V_2O_6)$ of 9.1×10^{-3} agrees well the $\gamma(V_2O_6)$ of 6×10^{-3} from Table 3, especially considering that a

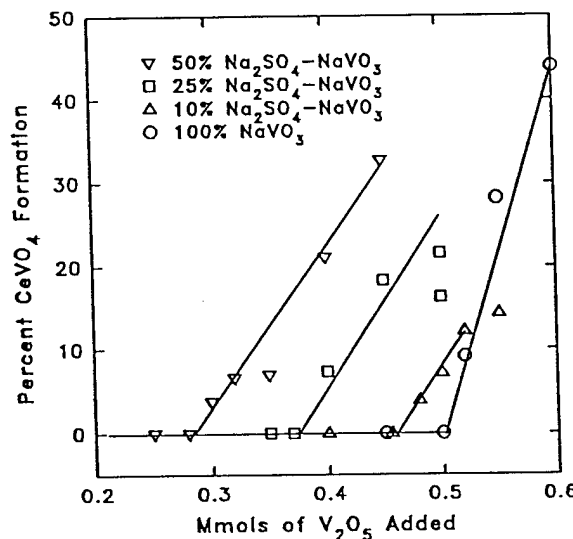


Fig. 12 Mmols V_2O_6 required for $CeVO_4$ formation at 800°C vs. $NaVO_3$ - Na_2SO_4 melt composition.

linear interpolation was applied to the Table 2 data. A datum point of $\gamma(V_2O_6) = 6 \times 10^{-3}$, $X(V_2O_6) = 0.1031$ with an error bar corresponding to ± 10 kJ error in $\Delta G^\circ_{\text{reaction}}$, which is still the largest likely error, is included in Fig. 14 as representative of this experiment. As shown in the drawn square in Fig. 14, the three independent experimental techniques all give essentially the same $\gamma(V_2O_6)$ for V_2O_6 in the 0.1 mol-fraction concentration range.

TABLE 3

Millimoles of V_2O_6 Required for $CeVO_4$ Formation
as a Function of Na_2SO_4 Content of the Melt at 800°C

Nominal melt composition	Mmols V_2O_6 for $CeVO_4$ formation	Mol-fraction of V_2O_6	Final mol-fraction of Na_2SO_4	Act. Coeff. ¹ of V_2O_6
100% $NaVO_3$	0.51	0.1131	0.0	0.0055
$NaVO_3$ -(10 mol%) Na_2SO_4	0.46	0.1031	0.0897	0.0060
$NaVO_3$ -(25 mol%) Na_2SO_4	0.38	0.0868	0.2283	0.0071
$NaVO_3$ -(50 mol%) Na_2SO_4	0.29	0.0676	0.4662	0.0092

¹ Calculated for act. (V_2O_6) = 6.2×10^{-3}

When V_2O_6 is added to melts containing significant Na_2SO_4 , the back-reaction of Reaction [12] can occur, with $NaVO_3$ produced in the melt and SO_3 evolved. In a flowing air stream, where SO_3 is continually removed, there can be a major extent of back-reaction, with 50 mol% Na_2SO_4 - $NaVO_3$ being converted ~80% to $NaVO_3$ in 24 hrs at 750°C [19]. In quiescent furnace air, the degree of back-reaction is much less. Also the reaction kinetics are slow in comparison to most chemical reactions. In the present case, the CeO_2 is finely ground together and thoroughly mixed with the $NaVO_3$ - Na_2SO_4 - V_2O_6 blend before firing. Upon coming to temperature, there is rapid reaction to form stable $CeVO_4$, and since the CeO_2 is in excess of V_2O_6 , no residual V_2O_6 is left to undergo reaction with Na_2SO_4 in the melt (which is heated only 2 hrs). Error because of Na_2SO_4 reaction with residual V_2O_6 should therefore be negligible.

When the V_2O_6 activity coefficients from Table 3 are plotted against the mol-fraction of Na_2SO_4 , an essentially straight line is obtained (Fig. 13). Theoretical reasons as to why the line should be straight have not been developed. However, Figs. 12 and 13 contain two points which have not been explicitly shown before, and which are perhaps not intuitive. First, increasing the Na_2SO_4 content of the melt causes $\gamma(V_2O_6)$ to increase; that is, V_2O_6 reaction with CeO_2 (and presumably other ceramic oxides) occurs with less V_2O_6 required in the melt (or vanadium in the fuel). Second, small differences in the V_2O_6 activity coefficients are not negligible. A change in $\gamma(V_2O_6)$ of from 5.5×10^{-3} to 9.2×10^{-3} , although at first sight insignificant, in fact corresponds to a nearly 2X decrease from 0.51 mmols to

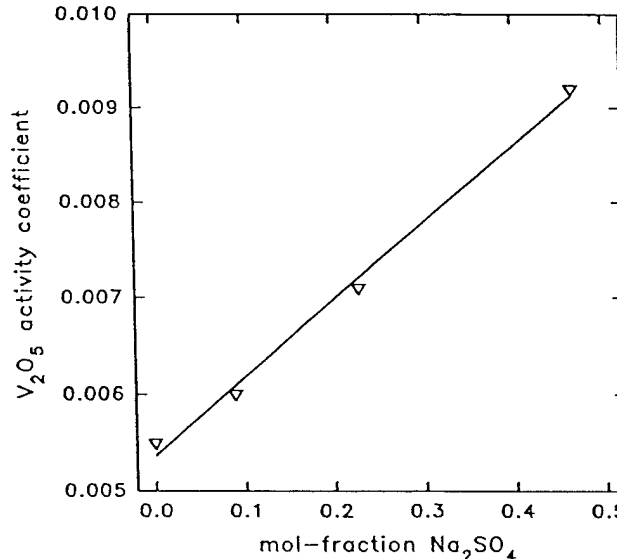


Fig. 13 Activity coefficient of V_2O_6 vs. mol-fraction of Na_2SO_4 at 800°C.

0.29 mmols in the amount of V_2O_6 required to reach the melt V_2O_6 activity at which CeO_2 will react or "corrode". In the service world, this could mean having to buy a fuel of half the vanadium content at considerably more expense.

SUMMARY AND CONCLUSIONS

Comparison with V_2O_6 Activity Coefficients from the Literature

The known V_2O_6 activity coefficients that have been reported for sodium vanadate, and sodium vanadate-sulfate mixtures, are shown in Fig. 14. The comparison is only qualitative, since the activity coefficients were measured with different melt conditions and temperatures. The Mittal and Elliott data point is calculated from their measurement of the activity of V_2O_6 in 0.5 mol-fraction $Na_2O \cdot V_2O_6$ (i.e., $NaVO_3$) at 850°C. The two Luthra and Spacil data points were reported for melts having a Na/V ratio of 2, and equilibrated under $p(SO_3)$'s of approximately 9×10^{-4} and 4×10^{-4} atm at 750°C and 900°C, respectively. Although Hwang and Rapp (23) originally postulated sodium sulfate-vanadate solutions to be ideal, a later paper by Rapp and Zhang (37) describes the equilibration of $Na_2SO_4 \cdot V_2O_6$ melts of varying Na/V ratio under a fixed $p(SO_3)$ of 2.2×10^{-3} bar at 900°C, and concludes that the melts are "-- close to an ideal salt solution although a small deviation seems to be present." No activity coefficient for V_2O_6 is given in their paper, but in a review of an NRL manuscript on vanadate-sulfates, a reviewer who seemed quite knowledgeable about the work stated that a V_2O_6 activity coefficient of 0.79 was indicated by the Rapp and Zhang results. So, despite its unusual derivation, this $\gamma(V_2O_6)$ is plotted in Fig. 14 for completeness of the comparison.

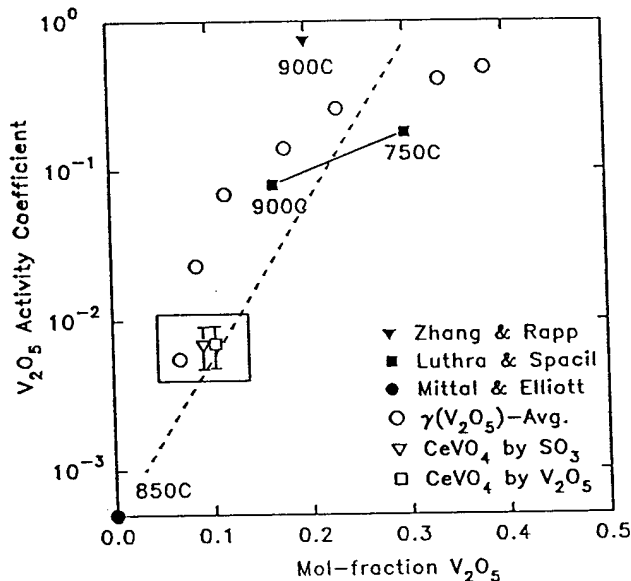


Fig. 14 Comparison of V_2O_6 activity coefficients from various works as plotted vs. mol-fraction of melt V_2O_6 .

Although somewhat scattered, the data in Fig. 14 exhibit a general trend of increase in $\gamma(V_2O_6)$ as the mol-fraction of V_2O_6 increases. Despite the difference in temperature, there is an essentially smooth transition between the $\gamma(V_2O_6)$ of $\sim 5 \times 10^{-4}$ (or $10^{-3.3}$) indicated by the Mittal and Elliott data for pure $NaVO_3$ at 850°C, and the $\gamma(V_2O_6)$ of $\sim 5 \times 10^{-3}$ determined from NRL results for an 800°C $NaVO_3$ melt containing 0.067 mol-fraction each of Na_2SO_4 and V_2O_6 . This is consistent with our expectations, considering that at this point only small increments of V_2O_6 have been added to pure $NaVO_3$. There is also reasonably good agreement with the Luthra and Spacil V_2O_6 activity coefficients of 0.08 and 0.18 in the middle regions of the plot, and with the 0.79 V_2O_6 activity coefficient of Rapp and Zhang for Na/V melts under high SO_3 partial pressures.

The three datum points within the drawn square are of particular importance. As described above, these points were determined by three independent experimental techniques, viz., simple equilibrium of $NaVO_3$ under SO_3 ; the reaction $CeO_2 + V_2O_6 \rightarrow CeVO_4 + 1/2 O_2$ where the V_2O_6 melt activity was increased by raising $p(SO_3)$; and the same reaction where V_2O_6 was simply "titrated" into the melt. Two different sets of thermodynamic data were also employed. Good agreement is seen

between the three values for $\gamma(V_2O_6)$ so obtained, which gives confidence that our experiments and data are essentially correct.

Other considerations

Effect of Na/V ratio in melt or engine deposit. In addition to $p(SO_3)$, the other principal variable in the $Na_2O-V_2O_6-SO_3$ system is the Na/V ratio. Information on the effect of the Na/V ratio is contained in our V_2O_6 "titration" experiments where blends of different $NaVO_3-Na_2SO_4$ ratios were investigated. For example, $NaVO_3$ -(50 mol%) Na_2SO_4 has a Na/V ratio of 3, and could be considered as approximating a melt that was originally Na_2O -(50 mol%) $NaVO_3$ (or Na_3VO_4), but in which the Na_2O component has been sulfated. Such an assumption is not unreasonable, since Na_2O has a considerably higher affinity for SO_3 than for V_2O_6 , as evidenced by the fact that the 800°C Na_2SO_4 dissociation activity product, $act.(Na_2O) \times act.(SO_3)$, is 9.8×10^{-21} , whereas the equivalent activity product for $NaVO_3$, $act.(Na_2O) \times act.(V_2O_6)$, is 1.7×10^{-18} . Taking this model to be indicative even if not totally correct, one can interpret the data in Fig. 13 as being for melts of Na/V ratios of 1, 1.22, 1.67 and 3.0, respectively, wherein $\gamma(V_2O_6)$ is found to progressively increase from 5.5×10^{-3} to 9.2×10^{-3} , or by 67%. Compared to the large changes in $\gamma(V_2O_6)$ produced by increasing $p(SO_3)$, this is relatively small, which suggests that $\gamma(V_2O_6)$ is not highly dependent upon the melt Na/V ratio, at least over the concentration ranges covered.

Vanadate-sulfate melts, ideal or nonideal? The data in Fig. 14 demonstrate that vanadate-sulfate melts are nonideal, and in fact follow a very common solution behavior wherein the melt components, when present in high concentration, behave as "nearly ideal", but when in dilute concentration, exhibit large negative deviations from ideal behavior, and have small activity coefficients.

ACKNOWLEDGEMENTS

The majority of our work was sponsored by the Office of Naval Research, with Dr. A. J. Sedriks as Scientific Officer. The financial support and intellectual encouragement that has been given in conjunction with this effort is gratefully acknowledged.

REFERENCES

1. W. T. Reid, *External Corrosion and Deposits: Boilers and Gas Turbines*, pgs. 134-138, American Elsevier, New York, 1971.
2. R. A. Miller, *Surf. Coat. Technol.* 30(1), 1 (1987).
3. R. L. Jones, "Thermal Barrier Coatings", in *Metallurgical and Ceramic Protective Coatings*, (ed. K. H. Stern), Chapman & Hall, New York, 1996.
4. W. P. Parks, E. E. Hoffman, W. Y. Lee and I. G. Wright, "Thermal Barrier Coatings Issues in Advanced Land-Based Gas Turbines," in *Proc. of Thermal Barrier Coating Workshop*, pg. 35-47, NASA Conf. Publ. 3312, NASA Lewis Research Center, OH (1995).
5. *Proc. of the Advanced Turbine Systems Annual Program Review Meeting*, DOE/OR-2048, (eds. A. Layne and P. Hoffman) U.S. Dept. of Energy, Washington DC, Nov., 1996.

6. J. F. Branthaver, "Influence of Metal Complexes in Fossil Fuels on Industrial Operations," in *Metal Complexes in Fossil Fuels: Geochemistry, Characterization and Processing*, pgs. 188-204 (eds. R. H. Filby and J. F. Branthaver) ACS Symp. Series 344, American Chemical Society, Washington, DC, 1987
7. R. L. Jones, *J. of Catalysis*, **129**, 269 (1991).
8. H. E. Hilliard, "Vanadium", in *Mineral Commodity Summaries*, 1997, U.S. Dept. of Interior, U. S. Geological Survey, Reston, VA, 1997.
9. *Proc. of 1st Conf. on Advanced Materials for Alternative Fuel Capable Directly Fired Heat Engines*, (eds. J. W. Fairbanks and J. Stringer), CONF-790749, U.S. Dept. of Energy, Washington, DC, 1979.
10. *Proc. of the 2nd Conf. on Advanced Materials for Alternative-Fuel-Capable Heat Engines*, (eds. J. W. Fairbanks and J. Stringer), RD-2369-SR, Electric Power Research Institute, Palo Alto, CA, 1982.
11. B. A. Nagaraj, A. F. Maricocchi, D. J. Wortman, J. S. Patton and R. L. Clarke, *ASME Paper 92-GT-44*, American Society of Mechanical Engineers, New York, 1992.
12. B. A. Nagaraj and D. W. Wortman, *Trans. ASME, J. Engr. for Gas Turbines and Power*, **112**, 536 (1990).
13. R. L. Jones, *J. Thermal Spray Technol.*, **6**[1], 77 (1997).
14. R. L. Jones, *Surf. Coat. Technol.*, **39/40**, 89 (1989).
15. D. W. Susnitzky, W. Hertl and C. B. Carter, *J. Am. Ceram. Soc.*, **71**[11], 992 (1988).
16. W. Hertl, *J. Appl. Phys.*, **63**[11], 5514 (1988).
17. A. N. Belov and G. A. Semenov, *Russ. J. Physical Chemistry*, **59**[3], 342 (1985).
18. H. Yokokawa, N. Sakai, T. Kawada and M. Dokiya, *J. Am. Ceram. Soc.*, **73**[3], 649 (1990).
19. R. L. Jones, C. E. Williams and S. R. Jones, *J. Electrochem. Soc.*, **133**[1], 227 (1986).
20. V. H. Schwarz and L. Schmidt, *Z. anorg. allg. Chem.*, **413**, 150 (1975).
21. K. L. Luthra and H. S. Spacil, *J. Electrochem. Soc.*, **129**[3], 649 (1982).
22. S. K. Mittal and J. F. Elliott, *J. Electrochem. Soc.*, **131**[5], 1194 (1984).
23. Y.-S. Hwang and R. A. Rapp, *Corrosion*, **45**[11], 933 (1989).
24. R. F. Reidy and R. L. Jones, *J. Electrochem. Soc.*, **142**[4], 1353 (1995).
25. M. Chaikivsky and C. W. Siegmund, *ASME Trans., J. Engr. for Power*, **87**, Series A, 379 (1965).
26. A. Block-Bolton and D. R. Sadoway, *Metall. Trans. B*, **14**, 231 (1983).

27. R. Mittelstadt and K. Schwerdtfeger, *Metall. Trans.*, **21B**, 111 (1990).
28. R. F. Reidy and K. E. Swider, *J. Am. Ceram. Soc.*, **78**(4), 1121 (1995).
29. D. W. Bonnell and J. W. Hastie, *High Temp. Science*, **26**, 313 (1990).
30. Y. K. Rao, *Stoichiometry and Thermodynamics of Metallurgical Processes*, pg. 825, Cambridge University Press, Cambridge, 1985.
31. "Phase diagram for V₂O₅-Na₂O System", Fig. 5126, *Phase Diagrams for Ceramists, Vol. IV*, (ed. G. Smith), The American Ceramic Society, Columbus, OH, 1981.
32. I. Barin, *Thermochemical Data of Pure Substances*, VCH Verlags Gesellschaft, Weinheim, 1989. As given in the commercial computer program, HSC Chemistry for Windows (Version 2.03)TM.
33. R. L. Jones, *J. Electrochem. Soc.*, **139**(10), 2794 (1992).
34. R. L. Jones, *J. Am. Ceram. Soc.*, **76**(6), 1635 (1993).
35. R. C. Kerby and J. R. Wilson, *Can. J. Chem.*, **51**, 1032 (1973).
36. H. K. Schmidt, *J. Am. Ceram. Soc.*, **70**(5), 367 (1987).
37. R. A. Rapp and Y. S. Zhang, "Electrochemical Studies of Hot Corrosion of Materials," in *Proc. of 1st Mexican Symp. on Metallic Corrosion*, Paper 12, pgs. 90-99, Meridan, Mexico, 7-11 March, 1994.